IIETA International Information and Engineering Technology Association
Advancing the World of Information and Engineering

Revue d'Intelligence Artificielle
Vol. 36, No. 5, October, 2022, pp. 801-807
Journal homepage: http://iieta.org/journals/ria

DermICNet: Efficient Dermoscopic Image Classification Network for Automated Skin Cancer Diagnosis

Sankarakutti Palanichamy Manikandan[1*], Vedanandam Karthikeyan[1], Ganesamoorthy Nalinashini[2]

[1] Department of ECE, DR. M.G.R Educational and Research Institute, Chennai, Tamilnadu-600095, India
[2] Department of EIE, R.M.D. Engineering College, Kavarapettai, Tamilnadu-601206, India

Corresponding Author Email: manikandansp17@gmail.com

https://doi.org/10.18280/ria.360519

Received: 26 May 2022
Accepted: 18 October 2022

Keywords:
computer aided diagnosis, deep learning architecture, dermoscopic image classification, neural networks, skin melanoma

ABSTRACT

The incidence of skin cancer is rapidly increasing worldwide. The relevance of Skin Cancer Diagnosis (SCD) and the difficulty in achieving an accurate and consistent diagnosis have resulted in significant research interest. Furthermore, automated detection or classification would be even more helpful in a diagnostic assistance system. This study develops an efficient Dermoscopic Image Classification Network (DermICNet) for automated SCD. The proposed DermICNet is a deep learning architecture with an efficient arrangement of eight convolutional layers with small-sized convolution filters (3x3). The extracted features from the convolution layers are fed to the dense layer for classification. It consists of a neural network that uses stochastic gradient descent optimization to find the optimal solution for SCD. Finally, a softmax classifier is employed to classify the patterns in the dermoscopic images. The proposed DermICNet is assessed using PH2 database images. The classification results reported are based on the random-split (70:30) approach, which divides the PH2 database into training and testing. It is demonstrated that it is feasible to discriminate between abnormal and normal dermoscopic images with an average accuracy of 99.2% using the proposed DermICNet. The results suggest that the analysis of dermoscopic images using DermICNet has the potential as a diagnostic tool for SCD.

1. INTRODUCTION

The extracted features of the skin lesion are vital elements of any image-based skin melanoma diagnosis support system. The critical diagnostic indicators or features for the clinical assessment of malignancy in melanoma include size, border irregularity, notching, boundary information, asymmetry, colour and textures [1-4]. A wide variety of automatic methods have been proposed based on colour or texture data with the help of conventional classification systems such as Support Vector Machine (SVM) [2], naïve Bayes [3], and k-nearest neighbour [4].

An efficient system is discussed in study [5] for SCD. It first segments the skin lesion using the k-means algorithm. Then colour and texture features are extracted, and a neural network is used for the classification. It also employs a feature reduction algorithm by t-test before classification. A hybrid model is discussed [6] for SCD that combines three multidirectional systems with a modified Multi-Layer Perceptron (MLP) for accurate classification. It uses sub-band energy features from shearlet, contourlet, and curvelet representation systems as features and exponentially weighted MLP is used for the classification.

Deep Convolutional Neural Network (DCNN) architecture-based SCD is discussed [7]. It uses Residual Network with 50 layers (ResNet50) to extract deep features. An improved grasshopper optimization is employed to reduce the feature space dimension, and then Naïve Bayes (NB) classifier is used for the classification. Another DCNN for SCD with different architecture is discussed [8]. It performs batch normalization with leaky rectified linear unit activation. A global average pooling layer is employed at the end of the architecture, followed by a fully connected layer for classifying different types of cancer using dermoscopic images.

Multi-Scale Multi CNN (MSM-CNN) is discussed in the study [9]. It uses different-resolution dermoscopic images with three DCNNs. An ensemble approach with three-level strategies is employed for effective classification. It fine tunes the CNNs with the help of batch normalization and dropout. Spatial domain features such as Asymmetry, Border, Color, and Diameter (ABCD), along with texture patterns by Gray Level Co-occurrence Matrix (GLCM), are discussed [10] for skin cancer classification. Eight abnormalities in dermoscopic images are classified using a Multi-class SVM (MSVM). A combination of LBP and a set of features in the study [10] is employed for skin cancer diagnosis [11]. Features are extracted from the segmented lesion obtained by the Otsu thresholding approach. It is a binary classification system that classifies dermoscopic images into two classes.

An efficient DCNN architecture is developed [12] for classifying the dermoscopic image into two classes. At first, the input data is normalized by z-score normalization. Then, a sigmoid layer-based DCNN with transfer learning is employed for the classification. A BI-Linear SK (BILSK) lesion classification system is discussed [13]. A bilinear architecture with transfer learning from ResNet50, Visual Geometry Group (VGG), and Xception is utilized for the classification. In the preprocessing stage, data augmentation and resizing of images are performed.

Eight EfficientNet architectures have been developed for

skin cancer classification in [14]. The architecture uses different batch sizes (from 4 to 32 in multiples of 2), learning rates, and optimizers such as Adam and stochastic gradient descent with varying decay rates. The fractal model system is discussed [15] for SCD. It uses a differential box-counting approach with both parametric (quadratic classifier) and non-parametric (Parzen classifier) for the classification.

An ensemble model is described [16] for SCD. The partial differential equations are used to remove hair, and a neural network model segment skin lesion. The correlation-based strategy is used to select the features from the retrieved characteristics such as colour, border, and texture features. A single hidden layer and two hidden layers' designs are used in the development of the ensemble model. An improved technique for the categorization of melanomas is described [17]. In the preprocessing stage, unwanted hair is removed using the Dull Razor technique, and then the contrast is increased. The Boltzman entropy is used to select features from shape, colour and texture, and a support vector machine (SVM) classifier is used to categorize those chosen features.

Soft computing methods, such as image processing, genetic algorithms and deep learning are utilized [18] to produce reliable classification results for SCD. First, dermoscopic pictures are preprocessed to remove noises and hairs. Second, three dimensional wavelet is employed for feature extraction and then feature selection by GA. Last, dermoscopic images are categorized using a deep learning classifier. The identification and classification of skin cancer utilizing an existing neural-based hybrid DL technique is described [19]. The ImageNet is a routine back propagation approach that combines AlexNet, VGG and GoogleNet for a robust system CNN model into a single NN architecture dealing with image classification.

The accuracy of the conventional SCD systems depends on the extracted features and the selected classifiers. The dominant features may fail due to the poor classifier and vice versa. Also, it requires two separate modules to design an accurate classification system. To overcome these difficulties, deep learning based architectures have been developed recently. The main objective of this work is to develop an efficient DCNN for an accurate and robust SCD system using dermoscopic images. The rest of the paper is organized as follows: Section 2 describes the proposed DermICNet for efficient SCD and Section 3 discusses the results obtained from the developed DermICNet model for skin melanoma classification. The conclusions and the future works are discussed in Section 4.

2. METHODS AND MATERIALS

Recently, there has been an interest in using deep learning techniques to classify skin cancer using dermoscopic images [12-14] and also in other medical image analysis systems, such as brain cancer [20], glaucoma [21] and lung cancer diagnosis [22, 23]. These techniques use pretrained networks and transfer learning to classify dermoscopic images. In this work, an efficient and new architecture is developed to achieve the highest classification accuracy than other pretrained networks. Figure 1 shows the developed deep learning architecture for skin melanoma classification.

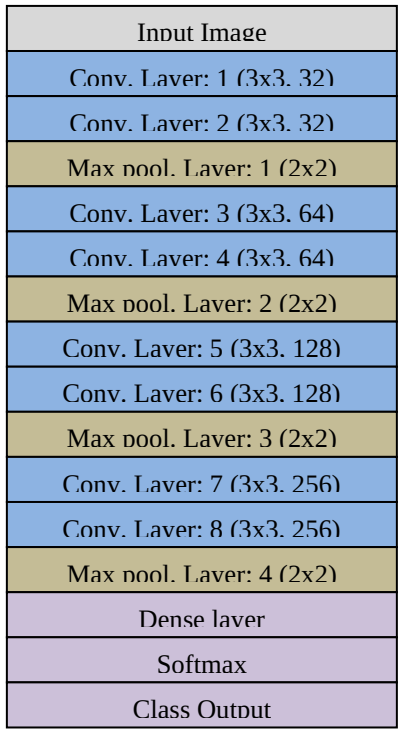

Figure 1. Proposed architecture of DermICNet

The deep learning architecture receives the dermoscopic image as input, and deep features are extracted. After extracting deep features, fully connected layers and an output layer are employed for the classification.

2.1 Deep feature extraction in DermICNet

In any deep learning architecture, two simple elements, such as convolution layers (feature extraction) and pooling layers (feature reduction), are employed for extracting deep features. For a given problem, the success of deep learning heavily depends on the arrangement of the abovementioned layers. In the convolution layer, the input image (x) is convolved with the convolution filter (h) (feature detector) to obtain the convolved image (y) (feature map) so that the fine details are extracted. The convolution operation is given by:

$$y(i,j) = \sum_{m=-\infty}^{\infty} \sum_{n=-\infty}^{\infty} h(m,n) \cdot x(i-m, j-n) \qquad (1)$$

Though the feature map size is the same as the input image size, using more convolution filters increases the input image's feature dimension. Before taking convolution, the element vector is flipped along the rows first and then along the columns. The flipping operation is shown in Figure 2 for sample convolution filter h. Figure 3 shows the convolution operation for a sample 5x5 image.

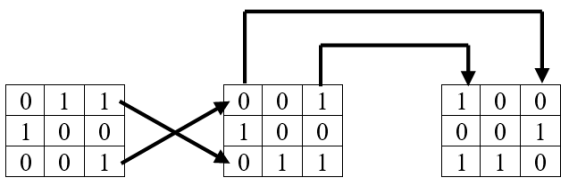

Figure 2. Flipping operations

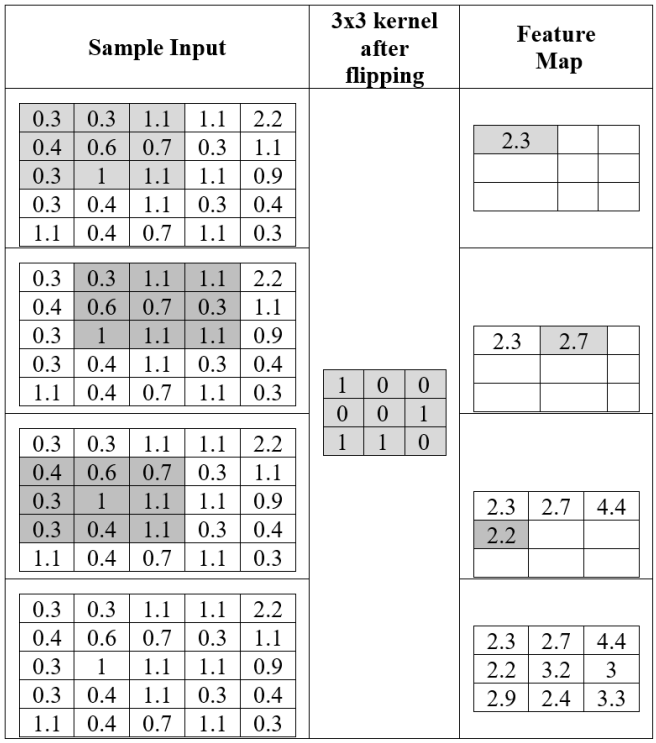

Figure 3. Convolution operation

In the first convolution layer, 32 convolution filters are used to extract the deep features from the dermoscopic image. This convolution operation increases the feature dimension to 32 times the resolution of the input image. The feature dimension is increased many times as the different number of filters is used in each layer. The term "stride" refers to the number of steps that are moved during each steps of the convolution process. It is set to one by default, and the same stride is employed in the proposed system.

To reduce the extracted feature dimension, the max pooling layer is utilized. The working of the max pooling layer is shown in Figure 4. It is observed from the Figure 4 that the feature dimension is reduced to half of the original dimension. To achieve this, a stride of 2 is used by the pooling layer in both movements, such as vertical and horizontal directions. Before applying the convolution and pooling operation, the dermoscopic image is normalized in [0-1].

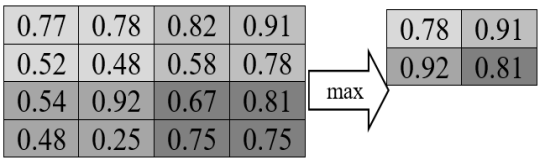

Figure 4. Feature reductions by max-pooling layer

2.2 Classification module in DermICNet

The fully connected layer in the DermICNet architecture is a classifier that classifies the input images into either normal or abnormal. This layer uses a Feed Forward Neural Network (FFNN) for the classification. They are often employed in classification tasks in various applications of the medial domain. Such models draw some inspiration from biological neural networks. Dimensionality problems are also known to affect the neural network models, and therefore the deep feature extraction stage employs a max pooling layer to reduce the dimensionality.

A FFNN consists of the input layer, the output layer and the hidden layers between them. Each layer has several neurons. Each neuron has its input, transfer function, and output, fully connected to the adjacent layer's neurons. The input layer receives the deep features from the previous module, and the output layer responds as either normal or abnormal. The hidden layers play a crucial part in processing the information. Once the number of layers and the number of neurons at each layer, i.e., the structure of FFNN, are determined, its performance depends on the transfer function of the neurons, the connection formula, and the learning rule.

All the signals arriving at a neuron are weighted, and combined to pass through a transfer function. The output for that neuron is then calculated. The Rectified Linear activation function (ReLU) is utilized in the input layer as it often provides better performances. The neuron gets the positive values only, and all negative values are discarded. This helps the network learn faster and overcomes the problem of vanishing gradient. The learning rule used in FFNN is the backpropagation algorithm. While training the network, the deep features from the training dermoscopic images are fed to FFNN to compute the weights between the neurons. To attain the specified accuracy, a loss function is introduced to optimize the weights by backward propagation. It is defined by:

$$CEL = -\sum_{j=1}^{c} t_c \log(p_c) \tag{2}$$

where, the probability for the i^{th} class is P_i and its truth label is t_i. In the output layer, softmax classifier is employed to classify the dermoscopic images into two classes. It is defined by:

$$p(O_i) = \frac{e^{O_i}}{\sum_{j=1}^{K} e^{O_j}} \tag{3}$$

where, K is the number of output layer, $p(O_i)$ is the probability of the i^{th} layer and O_i is the output of the i^{th} layer. The other important parameters used in FFNN are learning rate (0.001), max epochs (20), momentum (0.9) and batch processing is also employed.

3. RESULTS AND DISCUSSIONS

The results are obtained using the developed deep learning architecture on the PH2 database images [24, 25]. The PH2 database is one of the most popular available databases to researchers. It is employed in this work to test the superiority of DermICNet for classifying skin cancer images. The dermoscopic image is a 758 by 328 colour image, and there are 200 dermoscopic images available. It contains 40 melanomas of various tumour sizes, 80 atypical, and 80 common nevi examples. The PH2 database images are shown in Figure 5 and Table 1 shows the performance metrics used to show the effectiveness of the proposed system. The commonly used performance metrics [26, 27], such as accuracy, sensitivity and specificity are employed in this study.

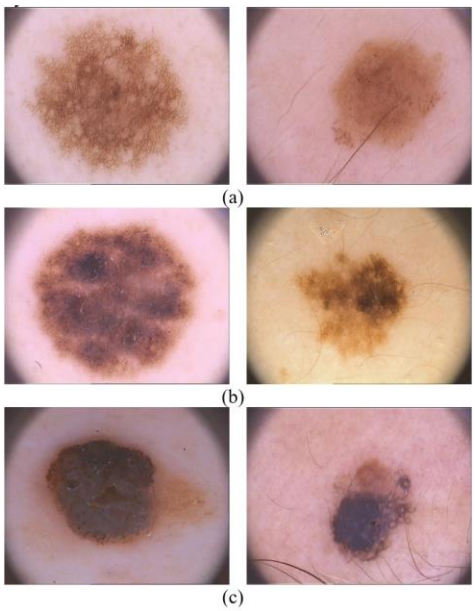

Figure 5. PH2 skin images: (a) Normal; (b) & (c) Abnormal

Table 1. Performance metrics of DermICNet for SCD

System output	Actual Class	
	Class-X	**Class-Y**
Class-X	#correct prediction of **Class-X** samples. (True Positive - *TP*)	#wrong prediction of **Class-Y** samples (False Positive -*FP*)
Class-Y	#wrong prediction of **Class-X** samples (False Negative-*FN*)	#correct prediction of **Class-Y** samples (True Negative-*TN*)
Performance measures	$S_n = \frac{TP}{TP+FN}$	$S_p = \frac{TN}{TN+FP}$
	$A_c = \frac{TP+TN}{TP+FN+TN+FP}$	

To attain better performance, the proposed DermICNet for SCD requires more images, so data augmentation [28-30] is employed. At first, the original image is rotated to 90, 180, and 270 degrees. Then the input image is flipped and again rotated into the degrees as mentioned above. This process creates seven more samples for an input image. Figure 6 shows the data augmented images and rescaled into 128 x 128 pixels to speed up the training process.

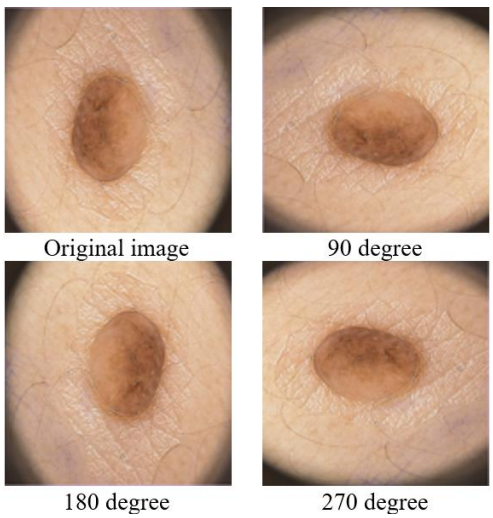

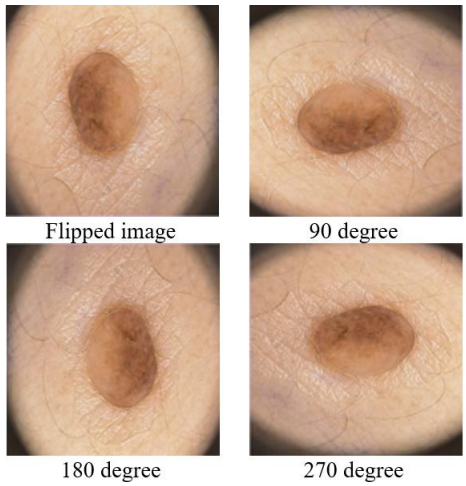

Figure 6. Data augmentation

3.1 Experimental parameters

This section summarizes the experimental parameters setting of the proposed DermICNet for SCD. Table 2 shows the parameter setting for SCD.

Table 2. Parameter settings of DermICNet for SCD

Parameters	Settings
Convolution filter size	3x3
Stride in convolution	1
Max pooling filter size	2x2
Stride in max pooling	2
Neural network	FFNN
Learning rate	0.0001
Momentum	0.9
Epochs	20
Normal images	80
Abnormal images	120
Augmentation	Yes (Rotation and Flipping)
Normal images (after augmentation)	640
Abnormal images (after augmentation)	960
Random split	70:30 (Training: Testing)

3.2 Performance analysis

The performance of the proposed DermICNet for SCD is analyzed in four ways; No Preprocessing + No Data Augmentation, Preprocessing + No Data Augmentation, No Preprocessing + Data Augmentation, Preprocessing + Data Augmentation. In preprocessing, a simple median filter is employed to remove the noises. The performances of the proposed DermICNet for SCD are shown in Table 3. This study also uses commonly used random split (70:30) for making training and testing sets.

Table 3. Performance of the proposed DermICNet for SCD

No.	Combination		Performance measure (%)		
	Preprocessing	**Data augmentation**	***Ac***	***Sn***	***Sp***
1	No	No	86.7	**88.9**	83.3
2	Yes	No	91.7	**91.7**	91.7
3	No	Yes	96.7	**97.6**	95.3
4	Yes	Yes	99.2	**99.3**	98.9

It is inferred from Table 3 that the proposed DermICNet provides a better performance of 99.2% accuracy when the input image is preprocessed with augmented images. It is also observed that preprocessing the images improves the performances of the DermICNet for SDC. The system's performance is improved by 5% when using the preprocessed original images after rescaling, and for augmented images, it is 10%. With preprocessing, the augmented images achieve a gain of 7.5% more than the original image. This is because some of the unwanted information that reduces the system performance is removed while preprocessing the images. The best combination provides 99.3% of sensitivity and 99% of specificity. Figure 7 shows the confusion matrices of DermICNet for SDC using the combinations discussed in Table 3. Figure 8 shows the training progress for all combinations with the cross entropy loss. In Figure 7, '0' represents the abnormal class and '1' represents the normal class.

Table 4 shows the comparative analysis of proposed DermICNet with other systems. The performance of the proposed system is compared with the following latest machine learning and deep learning based methods: contourlet & Bayesian [3], wavelet + statistical model & neural network [5], hybrid model & multilayer Perceptron [6], fractal model & probabilistic classifier [15], colour and textures & ensemble of neural networks [16], colour and textures & SVM [17], wavelet & deep learning [18] and colour and textures & Ensemble of CNN [19].

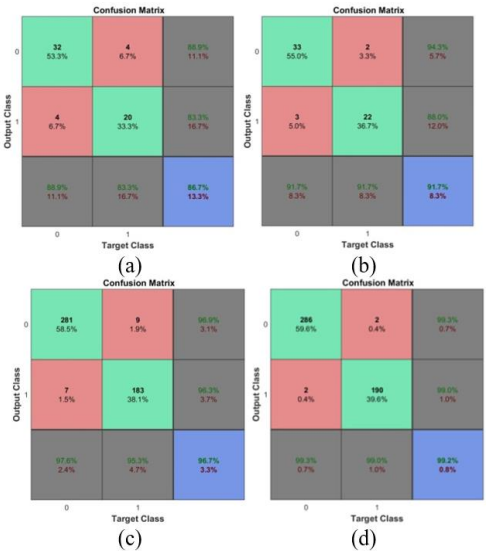

Figure 7. Confusion matrices of DermICNet for SDC: (a) No Preprocessing + No Data Augmentation; (b) Preprocessing + No Data Augmentation; (c) No Preprocessing + Data Augmentation; and (d) Preprocessing + Data Augmentation

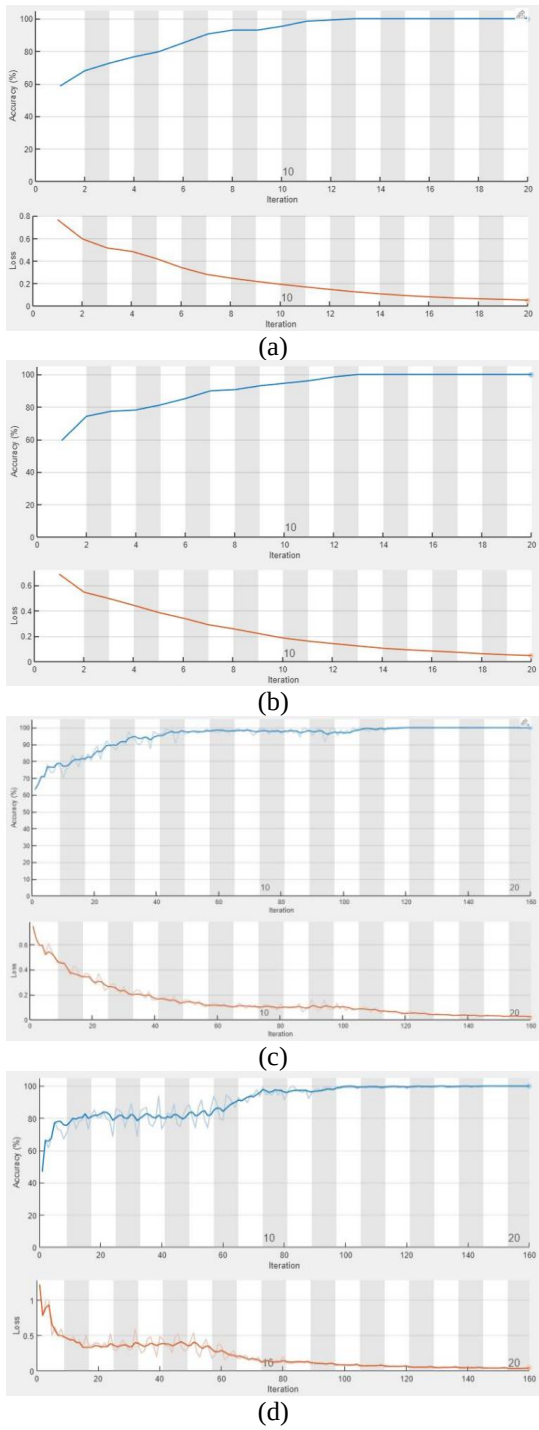

Figure 8. Training process: (a) No Preprocessing + No Data Augmentation; (b) Preprocessing + No Data Augmentation; (c) No Preprocessing + Data Augmentation; and (d) Preprocessing + Data Augmentation

Table 4. Comparative analysis with other systems

Features	Classifier	Sensitivity	Specificity	Accuracy
Contourlet [3]	Bayesian classifier	97.5	96.3	96.7
Wavelet + statistical model [5]	Neural network	90.83	95	92
Hybrid model [6]	Multilayer Perceptron	97.50	98.75	98.33
Fractal model [15]	Probabilistic classifier	95.8	93.8	95
Colour and textures [16]	Ensemble of neural networks	83.3	95	91.1
Colour and textures [17]	SVM	97.7	96.7	97.5
Wavelet [18]	Deep learning	98.33	99.03	98.67
Colour and textures [19]	Ensemble of CNN	93	84	-
Proposed system		**99.3**	**98.9**	**99.2**

It can be shown from Table 4 that the categorization of melanoma skin cancer images utilizing the DermICNet delivers the greatest performance compared to other relevant research for SCD.

4. CONCLUSIONS

In this work, the concept of CNN is used to develop the proposed DermICNet for classifying dermoscopic images as normal or abnormal. The developed DermICNet for SDC is analyzed with different combinations of preprocessing and data augmentation. The former step removes the noises, and the later step increases the samples to attain better accuracy. It is observed that the proposed DermICNet for SDC provides promising results when using preprocessed and augmented images as inputs to the system. The average accuracy of the proposed DermICNet (99.2%) is much higher than others. It is observed that the proposed DermICNet has a potential role explicitly to play in classifying dermoscopic images. In the future, the inception module can be used to further increase the system's performance. It is a powerful architecture that allows parallel learning from parallel convolution filters of different or the same sizes.

REFERENCES

[1] Stolz, W., Riemann, A., Cognetta, A. (1994). ABCD rule of dermatoscopy: A new practical method for early recognition of malignant melanoma. European Journal of Dermatology, 4: 521-527. https://doi.org/10.1016/S0190-9622(94)70061-3

[2] Mohan Kumar, S., Kumanan, T. (2021). Dermoscopic image classification using two-stage processing of shearlet features with support vector machine. In: Sharma, D.K., Son, L.H., Sharma, R., Cengiz, K. (eds) Micro-Electronics and Telecommunication Engineering. Lecture Notes in Networks and Systems. https://doi.org/10.1007/978-981-33-4687-1_43

[3] Sonia, R. (2016). Melanoma image classification system by NSCT features and Bayes classification. International Journal of Advances in Signal and Image Sciences, 2(2): 27-33. https://doi.org/10.29284/ijasis.2.2.2016.27-33

[4] Ganster, H., Pinz, P., Rohrer, R., Wildling, E., Binder, M. (2001). Automated melanoma recognition. IEEE Transaction on Medical Imaging, 20: 233-239. https://doi.org/10.1109/42.918473

[5] Thamizhamuthu, R., Manjula, D. (2021). Skin melanoma classification system using deep learning. Computers, Materials & Continua, 68(1): 1147-1160. https://doi.org/10.32604/cmc.2021.015503

[6] Vidya Lakshmi, V., Leena Jasmine, J.S. (2021). A hybrid artificial intelligence model for skin cancer diagnosis. Computer Systems Science and Engineering, 37(2): 233-245. https://doi.org/10.32604/csse.2021.015700

[7] Afza, F., Sharif, M., Mittal, M., Khan, M.A., Hemanth, D.J. (2022). A hierarchical three-step superpixels and deep learning framework for skin lesion classification. Methods, 202: 88-102. https://doi.org/10.1016/j.ymeth.2021.02.013

[8] Iqbal, I., Younus, M., Walayat, K., Kakar, M.U., Ma, J. (2021). Automated multi-class classification of skin lesions through deep convolutional neural network with dermoscopic images. Computerized Medical Imaging and Graphics, 88: 101843. https://doi.org/10.1016/j.compmedimag.2020.101843

[9] Mahbod, A., Schaefer, G., Wang, C., Dorffner, G., Ecker, R., Ellinger, I. (2020). Transfer learning using a multi-scale and multi-network ensemble for skin lesion classification. Computer Methods and Programs in Biomedicine, 193: 105475. https://doi.org/10.1016/j.cmpb.2020.105475

[10] Monika, M.K., Vignesh, N.A., Kumari, C.U., Kumar, M.N., Lydia, E.L. (2020). Skin cancer detection and classification using machine learning. Materials Today: Proceedings, 33: 4266-4270. https://doi.org/10.1016/j.matpr.2020.07.366

[11] Tumpa, P.P., Kabir, M.A. (2021). An artificial neural network based detection and classification of melanoma skin cancer using hybrid texture features. Sensors International, 2: 100128. https://doi.org/10.1016/j.matpr.2020.07.366

[12] Ali, M.S., Miah, M.S., Haque, J., Rahman, M.M., Islam, M.K. (2021). An enhanced technique of skin cancer classification using deep convolutional neural network with transfer learning models. Machine Learning with Applications, 5: 100036. https://doi.org/10.1016/j.mlwa.2021.100036

[13] Calderón, C., Sanchez, K., Castillo, S., Arguello, H. (2021). BILSK: A bilinear convolutional neural network approach for skin lesion classification. Computer Methods and Programs in Biomedicine Update, 1: 100036. https://doi.org/10.1016/j.cmpbup.2021.100036

[14] Ali, K., Shaikh, Z.A., Khan, A.A., Laghari, A.A. (2021). Multiclass skin cancer classification using efficientnets–A first step towards preventing skin cancer. Neuroscience Informatics, 100034. https://doi.org/10.1016/j.neuri.2021.100034

[15] Jacob, S., Rosita, J.D. (2021). Fractal model for skin cancer diagnosis using probabilistic classifiers. International Journal of Advances in Signal and Image Sciences, 7(1): 21-29. https://doi.org/10.2312/LocalChapterEvents/TPCG/TPCG09/041-048

[16] Xie, F., Fan., H., Li, Y., Jiang, Z., Meng, R., Bovik, A. (2016). Melanoma classification on dermoscopy images using a neural network ensemble model. IEEE Transactions on Medical Imaging, 36(3): 849-858. https://doi.org/10.1109/TMI.2016.2633551

[17] Nasir, M., Attique Khan, M., Sharif, M., Lali, I.U., Saba, T., Iqbal, T. (2018). An improved strategy for skin lesion detection and classification using uniform segmentation and feature selection based approach. Microscopy Research and Technique, 6: 528-543. https://doi.org/10.1002/jemt.23009

[18] Maniraj, S.P., Sardarmaran, P. (2021). Classification of dermoscopic images using soft computing techniques. Neural Computing and Applications, 33(19): 13015-13026. https://doi.org/ 10.1007/s00521-021-05998-5

[19] Mahbod, A., Schaefer, G., Ellinger, I., Ecker., R., Pitiot A.,Wang, C. (2019). Fusing fine-tuned deep features for skin lesion classification. Computerized Medical Imaging and Graphics, 71: 19-29. https://doi.org/10.1016/j.compmedimag.2018.10.007

[20] Muthaiyan, R., Malleswaran, D.M. (2022). An automated brain image analysis system for brain cancer using shearlets. Computer Systems Science and

Engineering, 40(1): 299-312. https://doi.org/10.32604/csse.2022.018034
[21] Pin, K., Chang, J.H., Nam, Y. (2022). Comparative study of transfer learning models for retinal disease diagnosis from fundus images. Computers, Materials & Continua, 70(3): 5821-5834. https://doi.org/10.32604/cmc.2022.021943
[22] Shimazaki, A., Ueda, D., Choppin, A., Yamamoto, A., Honjo, T., Shimahara, Y. Miki, Y. (2022). Deep learning-based algorithm for lung cancer detection on chest radiographs using the segmentation method. Scientific Reports, 12(1): 1-10. https://doi.org/10.1038/s41598-021-04667-w
[23] Ramitha, M.A., Mohanasundaram, N. (2021). Classification of pneumonia by modified deeply supervised resnet and senet using chest x-ray images. International Journal of Advances in Signal and Image Sciences, 7(1): 30-37. https://doi.org/10.29284/ijasis.7.1.2021.30-37
[24] Mendonça, T., Ferreira, P.M., Marques, J.S., Marcal, A.R., Rozeira, J. (2013). PH2-A dermoscopic image database for research and benchmarking. 35th Annual International Conference on Engineering in Medicine and Biology Society, pp. 5437-5440. https://doi.org/10.1109/EMBC.2013.6610779
[25] PH2 Database Link: https://www.fc.up.pt/addi/ph2%20database.html
[26] Hicks, S.A., Strümke, I., Thambawita, V., Hammou, M., Riegler, M.A., Halvorsen, P., Parasa, S. (2022). On evaluation metrics for medical applications of artificial intelligence. Scientific Reports, 12(1): 1-9. https://doi.org/10.1038/s41598-022-09954-8
[27] Müller, D., Soto-Rey, I., Kramer F.,(2022). Towards a guideline for evaluation metrics in medical image segmentation. BMC Res Notes, 15: 210. https://doi.org/10.1186/s13104-022-06096-y
[28] Jia, S.J., Wang, P., Jia, P.Y., Hu, S.P. (2017). Research on data augmentation for image classification based on convolution neural networks. Chinese Automation Congress, Jinan, China, pp. 4165-4170. https://doi.org/10.1109/CAC.2017.8243510
[29] Mikołajczyk, A., Grochowski, M. (2018). Data augmentation for improving deep learning in image classification problem. International Interdisciplinary PhD Workshop, 117-122. https://doi.org/10.1109/IIPHDW.2018.8388338
[30] Shorten, C., Khoshgoftaar, T.M. (2019). A survey on image data augmentation for deep learning. Journal of Big Data, 6(1): 1-48. https://doi.org/10.1186/s40537-019-0197-0

NOMENCLATURE

h	convolution filter
Ac	accuracy
Sn	sensitivity
Sp	specificity
p	probability